Inorganic Chemistry

Article

pubs.acs.org/IC

Determination of Crystal-Field Energy Levels and Temperature Dependence of Magnetic Susceptibility for Dy^{3+} in $[Dy_2Pd]$ Heterometallic Complex

Mirosław Karbowiak,*[,†] Czesław Rudowicz,[‡] and Takayuki Ishida[§]

[†]Faculty of Chemistry, University of Wrocław, ul. F. Joliot-Curie 14, 50-383 Wrocław, Poland

[‡]Institute of Physics, West Pomeranian University of Technology, Szczecin, Poland

[§]Department of Engineering Science, The University of Electro-Communications, Tokyo 182-8585, Japan

Supporting Information

ABSTRACT: This study is the first in a series of experimental and theoretical investigations of the crystal-field (CF) energy levels obtained from optical electronic spectra for selected heterometallic 4f-3d compounds intensively studied for the development of novel single-molecule magnets (SMMs). An intriguing question is why the $[\{Dy^{III}(hfac)_3\}_2Cu^{II}(dpk)_2]$ (abbreviated as $[Dy_2Cu]$; Hhfac = 1,1,1,5,5,5-hexafluoropentane-2,4-dione, Hdpk = di-2-pyridyl ketoxime) has antiferromagnetic coupling, whereas $[Gd_2Cu]$ and heavy $[Ln_2Cu]$ systems usually show ferromagnetic coupling. As the first step to explain this peculiarity, the recently synthesized complex, $[Dy_2Pd]$, is investigated. This complex is isostructural with $[Dy_2Cu]$ yet contains the diamagnetic Pd ion instead of the magnetic Cu(II) ion. Experimental energy levels of Dy^{3+} ions in the powder $[Dy_2Pd]$ sample were determined from the 4.2 K absorption spectra. CF analysis was performed yielding the fitted free ion and CF parameters. The number of freely varied parameters was restricted using the superposition model. The fittings yield very satisfactory agreement between the experimental and the calculated energy levels (*rms* = 12.0 cm^{-1}). The energies and exact composition of the state vector for the ground multiplet $^6H_{15/2}$ of Dy^{3+} are determined. These results are used for the simulation of the temperature dependence of the magnetic susceptibility, which enables the theoretical interpretation of the experimentally measured magnetic susceptibility in the range 1.8−300 K for the $[Dy_2Pd]$ complex. This study provides background for the subsequent investigation of the magnetic exchange interactions in the pertinent heterometallic complexes.

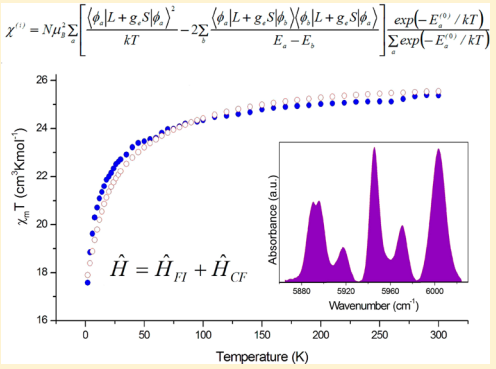

INTRODUCTION

Single-molecule magnets (SMMs) exhibit magnetic hysteresis, that is, extremely slow magnetization reversal because of a high energy barrier. Individual molecules, usually with high spin because of significant exchange couplings among the constituent ions, that function as nanoscale magnetic particles are considered as SMMs.[1−3] The new notion of single-ion magnets (SIMs) has recently been introduced to distinguish the SMMs from the systems in which the slow relaxation is not associated to intramolecular coupling, like in SMMs, but it is associated to single ion behavior.[4] In the mononuclear lanthanoid SMM, or rather SIM complexes, magnetic properties are directly related to the crystal-field (CF) created on the 4f ions by the surrounding ligands.[5−8] The properties of polynuclear SMMs are driven by the exchange coupling between 4f and 3d spins. Andruh et al.[8] considered the interplay between such couplings and the crystal field effects in Gd−Cu complexes. Synthetic strategies and magnetic properties of the heterometallic 3d-4f complexes, which are of high interest in molecular magnetism, have been presented in the review.[8] It appears that the knowledge of the energy level structure of ground and excited configurations of Ln(III) ions and thus the CF parameters (CFPs) is a prerequisite for understanding and modeling of properties of both mono- and poly nuclear SMMs.[5−8] This is because the magnetic properties of the most rare-earth ions are strongly influenced by the orbital component of the magnetic moment, because of spin−orbit coupling of the f electrons compared with the ligand-field effects. Moreover, the ligand-field effects and the exchange interactions between the magnetic centers become relevant at the same temperature range. It has been emphasized[8] that it is necessary to gather a large number of experimental data to evaluate the CF effects of each individual Ln^{3+} ion and to gain insight into the low-lying levels. Hence information on multiplet splitting in a 4f-electronic system is of crucial importance for studying and understanding magnetic properties of a lanthanide complex.[9]

Apart from the importance of empirical evaluation of the CF (or ligand-field) effects on the magnetic properties, several

Received: August 22, 2013
Published: November 4, 2013

dx.doi.org/10.1021/ic4021542 | *Inorg. Chem.* 2013, 52, 13199−13206

other key aspects, which seem worth considering, have been identified.[8,9] Since consideration of these aspects is planned in subsequent papers, they are categorized as follows. (i) The importance of the magnetostructural correlations, namely, from the structural determinations and magnetic studies, a correlation has been found between the value of the ferromagnetic interaction J and the dihedral angle, α, between the two planes (OCuO and OGdO) involving the bridging oxygen atoms and each metal ion in doubly oxo-bridged Gd−Cu systems. Such correlations and the pertinent CF data may help identifying some differences between the ferromagnetic (F) and antiferromagnetic (AF) 3d-4f complexes, which could explain the "odd" behavior of $[\{Dy^{III}(hfac)_3\}_2Cu^{II}(dpk)_2]$ (abbreviated as $[Dy_2Cu]$ hereafter) (AF) complex as compared with other heavy-lanthanide $[Ln_2Cu]$ (Ln = Gd, Tb, Ho) (F) complexes[10] (Hhfac = 1,1,1,5,5,5-hexafluoropentane-2,4-dione, Hdpk = di-2-pyridyl ketoxime; Scheme 1 for the molecular

Scheme 1. Structural Formula

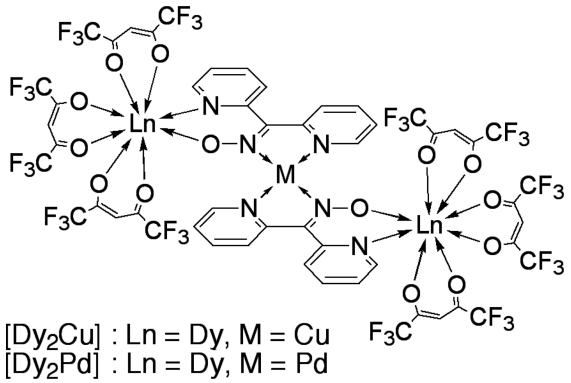

structure). Even if such crystals are structurally similar, like $[Dy_2Pd]$ and $[Dy_2Cu]$ are completely isomorphous, some subtle structural differences between the F-tic and AF-tic 3d-4f complexes may be revealed. (ii) The role of the Ln orbitals, namely, the theoretical work directed toward the mechanism of ferromagnetic coupling in Cu−Gd complexes has evidenced the active role played by the ligand and by the empty 5d Gd orbitals slightly hybridized with the 4f orbitals via a spin-polarization effect transmitted by the ligand, whereas the dominating role of a structural factor is a strong experimental argument in favor of a decisive contribution of the 5d Gd orbitals in the magnetism of the Cu−Gd complexes. These ideas may provide a clue for the observed differences between the F-tic and AF-tic 3d-4f complexes.[11] (iii) The role of the magnetic $3d^N$ ions in the heterometallic 3d-4f complexes, namely, the trends in the expected J values in going from one $3d^N$ ion to another, resulting from the decrease of the exchange mechanism (J values) with the increasing number of active 3d electrons in going from copper to nickel, cobalt, and iron. (iv) The trends in the CFPs across the $4f^N$ series for a series of isostructural lanthanide complexes, for example, each CFP was assumed[9] to be a linear function of atomic number of the lanthanide. Establishment of such trends may provide information on CFPs for systems for which complete spectroscopic data are not yet available.

Various approaches based on a parametric Hamiltonian have been employed to derive the CF energy levels structure of Ln(III) ions in heterometallic 4f-3d compounds,[4−9] which have been intensively studied for development of novel SMMs.[12] It is especially difficult if the experimental energies cannot be obtained from the f-f electronic transitions using optical spectroscopy. To overcome this difficulty, Ishikawa et al.[9] utilized an algorithm to search for the CFP sets simultaneously reproducing both paramagnetic shifts of ^{1}H NMR spectra and temperature dependence of magnetic susceptibility. Baldovi et al.[7b] used the Radial Effective Charge (REC) model, based on the crude point-charge model, to obtain the CFPs, the energy level scheme, and the associated wave functions. Note that some terminological confusion has inadvertently crept into the papers.[4,7a,b] Clarification of this confusion is beyond the scope of this paper and will be provided in a separate review.

Importantly some of the heterometallic compounds synthesized and characterized by Ishida and co-workers[12] are much related to the single ion magnets (SIMs).[4,7] In many cases, the lanthanide complexes have square-antiprism structures around Ln when Ln is eight-coordinated. The major interest is in the exchange coupling between 4f and 3d ions, for example, Ln-Cu, Ln-Ni. However, the characteristics, that is, the activation energy for magnetization reversal (E_a) and macroscopic quantum tunneling of magnetization (QTM) in the molecular nanomagnets of the type SMM or SIM, may be dominantly regulated by the Ln crystal field and accordingly by the single-ion anisotropy.[4,7,8] In view of the SIM strategy the distortion from the ideal square-antiprism in the 4f-3d heterometallic systems seems important since it affects the exchange couplings. Actually the 4f-3d systems often become SMMs. A possible reason may reside in the presence of a bias field at the Ln site, namely, the Ln ion feels the exchange coupling from the 3d ion spin. It can be regarded as an "exchange field" at the Ln site,[13] which disables the Ln ion from undergoing zero-field QTM. This effect will raise the empirical E_a and decrease the probability of QTM. Therefore, the studies of the mechanism of SIMs are timely and important.

This paper is the first in a series of experimental and theoretical investigations of selected heterometallic 4f-3d compounds. A general approach based on the CF analysis (CFA) and superposition model (SPM), which has been extensively utilized for Ln ions in low symmetry crystals,[14] is employed here. The CFPs are first modeled using SPM and structural data and then experimentally determined from the CF energy levels obtained from optical electronic spectra for selected heterometallic 4f-3d compounds. The combined CFA/SPM approach enables to gain better insight into the spectroscopic and magnetic properties of the Dy^{3+} ions in the heterometallic $[Dy_2Pd]$ complex. An intriguing question is why $[Dy_2Cu]$ has antiferromagnetic coupling,[10] whereas $[Gd_2Cu]$ and heavy $[Ln_2Cu]$ systems usually show ferromagnetic coupling. As the first step to explain this peculiarity, we study the $[Dy_2Pd]$ complex, which is isostructural with $[Dy_2Cu]$.[15] Experimental energy levels of Dy^{3+} ions in the powder $[Dy_2Pd]$ sample determined from the 4.2 K absorption spectra are presented in the next Section. CF analysis was performed, and the fitted free ion and CF parameters were determined. The number of freely varied parameters was restricted using the superposition model. The fittings yield very satisfactory agreement between the experimental and the calculated energy levels (rms = 11.0 cm^{-1}). The energies and exact composition of the state vector for the ground multiplet $^6H_{15/2}$ of Dy^{3+} are also determined. These results are used for simulation of temperature dependence of magnetic susceptibility, which enables theoretical interpretation of the experimentally measured magnetic susceptibility for the $[Dy_2Pd]$ complex.

dx.doi.org/10.1021/ic4021542 | Inorg. Chem. 2013, 52, 13199−13206

This study provides background for subsequent investigation of the exchange interactions in the pertinent heterometallic complexes.

EXPERIMENTAL SECTION

Synthesis. [{Dy(hfac)$_3$}$_2$Pd(dpk)$_2$] was prepared as described elsewhere.[15]

Optical Electronic Spectra. Absorption spectra were recorded in the 3500−50000 cm^{-1} range at 4.2 K on a Cary-5000 UV−vis−NIR spectrophotometer, equipped with an Oxford Instrument model CF1204 cryostat.

Magnetic Susceptibility. Magnetic susceptibility of polycrystalline specimens of [Dy$_2$Pd] was measured on a Quantum Design MPMS-7 SQUID magnetometer, equipped with a 7 T coil, in a temperature range 1.8−300 K. The magnetic responses were corrected with diamagnetic blank data of the sample holder measured separately. The diamagnetic contribution of the sample itself was estimated from Pascal's constants.

The theoretical temperature dependence of magnetic susceptibility corresponding to a given principal axis i (x, y, z) may, in general, be calculated using the Van Vleck formula, eq 1,[16] where N is the

$$\chi^{(i)} = N\mu_B^2 \sum_a \left[\frac{\langle \phi_a | L + g_e S | \phi_a \rangle^2}{kT} - 2 \sum_b \frac{\langle \phi_a | L + g_e S | \phi_b \rangle \langle \varphi_b | L + g_e S | \phi_a \rangle}{E_a - E_b} \right] \frac{\exp(-E_a^{(0)}/kT)}{\sum_a \exp(-E_a^{(0)}/kT)} \quad (1)$$

Avogadro number, μ_B is the Bohr magneton, and k is the Boltzmann constant. The wave functions unperturbed by the external magnetic field, denoted as ϕ_a and ϕ_b, correspond to the eigenvalues E_α, that is, the energy levels, obtained from diagonalization of the CF Hamiltonians discussed in following sections. The expectations predicted based on eq 1 were used to calculate the theoretical average susceptibility: $\chi_{av} = (\chi^{(x)} + \chi^{(y)} + \chi^{(z)})/3$, which is then compared with the experimental curves obtained for the powder sample investigated in this study.

RESULTS

Optical Absorption Measurements. Figure 1 shows the survey absorption spectrum of the powder [Dy$_2$Pd] sample. The well resolved lines observed in the region of 4000−18000 cm^{-1} enable assignment of CF components of seven among nine possible lowest energy $^{2S+1}L_J$ multiplets. The absorption transitions to the ^{6}H$_{13/2}$ multiplet are expected at about 3500−3700 cm^{-1} but could not be identified in the spectra, most probably because of overlapping with the absorption bands of the OH groups. Figure 2 presents the high resolution spectra corresponding to the transitions from the ground multiplet to the energy levels of ^{6}H$_J$ (J = 11/2, 9/2, 7/2, and 5/2) and ^{6}F$_J$ (J = 11/2, 9/2, 7/2, 5/2, and 3/2) excited multiplets. In total, the energies of 38 experimental levels were determined from analysis of absorption spectra. There is, however, an inherent limitation, which cannot be overcome, that is, the higher lying levels (above about 21000 cm^{-1}) are obscured by the absorption bands of the ligands (Figure 1). Thus, the number of the observed experimental energy levels, which could be used for CF fittings, was not too large. In spite of this limitation, the CF calculations yield quite reasonable results (see below). In this situation, the CF calculations for other Ln^{3+} ions in isostructural compounds would help to increase the reliability of the present results.

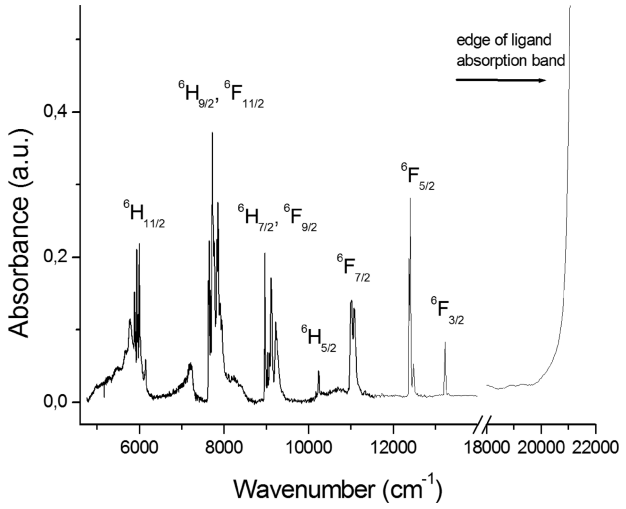

Figure 1. Survey absorption spectrum of the powder [Dy$_2$Pd] sample (thin film of sample dispersed in nujol oil) at 4.2 K. The labels denote the terminal multiplets for transitions originating from the ground ^{6}H$_{15/2}$ multiplet.

Structural Analysis. [Dy$_2$Pd] crystallizes in the monoclinic system with the space group $P2_1/n$, whereas each molecule has an inversion center at the Pd ion.[15] The lattice constants are [in nm]: a = 0.8282(2), b = 2.5075(14) and c = 1.5538(5), β = 91.255(5)° and Z = 2. The Dy^{3+} ions occupy only one atomic position with C_1 point symmetry. The original crystallographic coordinates (x, y, z) of atoms forming the coordination sphere of the central Dy^{3+} ion, extracted from the CIF files, are presented in the Supporting Information, Table S1. These coordinates are used in the SPM analysis. Since the original crystallographic axis system (CAS), defined by the axes (a, b, c), was not Cartesian, the orthogonalization was performed to obtain a Cartesian CAS* by setting the N3 atom (as numbered in CIF file) on the z-axis. The transformed crystallographic coordinates are listed in Supporting Information, Table S2, whereas the polar coordinates used in SPM analysis are listed in Table 1. The coordination of Dy^{3+} ions in the powder [Dy$_2$Pd] sample is presented in Figure 3.

SPM Calculations of CFPs. The theoretical background for these calculations and notation used for relevant parameters may be found in our previous papers.[14] The input values of the coordination factors[14a,b] listed in Supporting Information, Table S3 were obtained in the following way. The same distance for the atoms O2−O7 is assumed (clustering approximation). The oxygen atom O1 (from ketoxime) differs from O2−O7 (from β-diketonate). The axis system has been chosen in such a way that the N3 atom is located on the z-axis. Then the contributions from the N3 atom are only to the axial CF parameters: B_{20}, B_{40} and B_{60}. The contributions from O1 are included in the intrinsic parameters set denoted $B_k(a)$. The contributions from O2−O7 are included in the intrinsic parameters set denoted $B_k(b)$.

CF Analysis and Energy Level Calculations. Because of the low site symmetry of the Dy^{3+} ions in [Dy$_2$Pd], all energy levels are labeled by the same irreducible representations (irreps) and thus no specific selection rules exist for the electronic transitions, which generally depend on the incident light polarization. Hence, no additional information concerning

dx.doi.org/10.1021/ic4021542 | Inorg. Chem. 2013, 52, 13199−13206

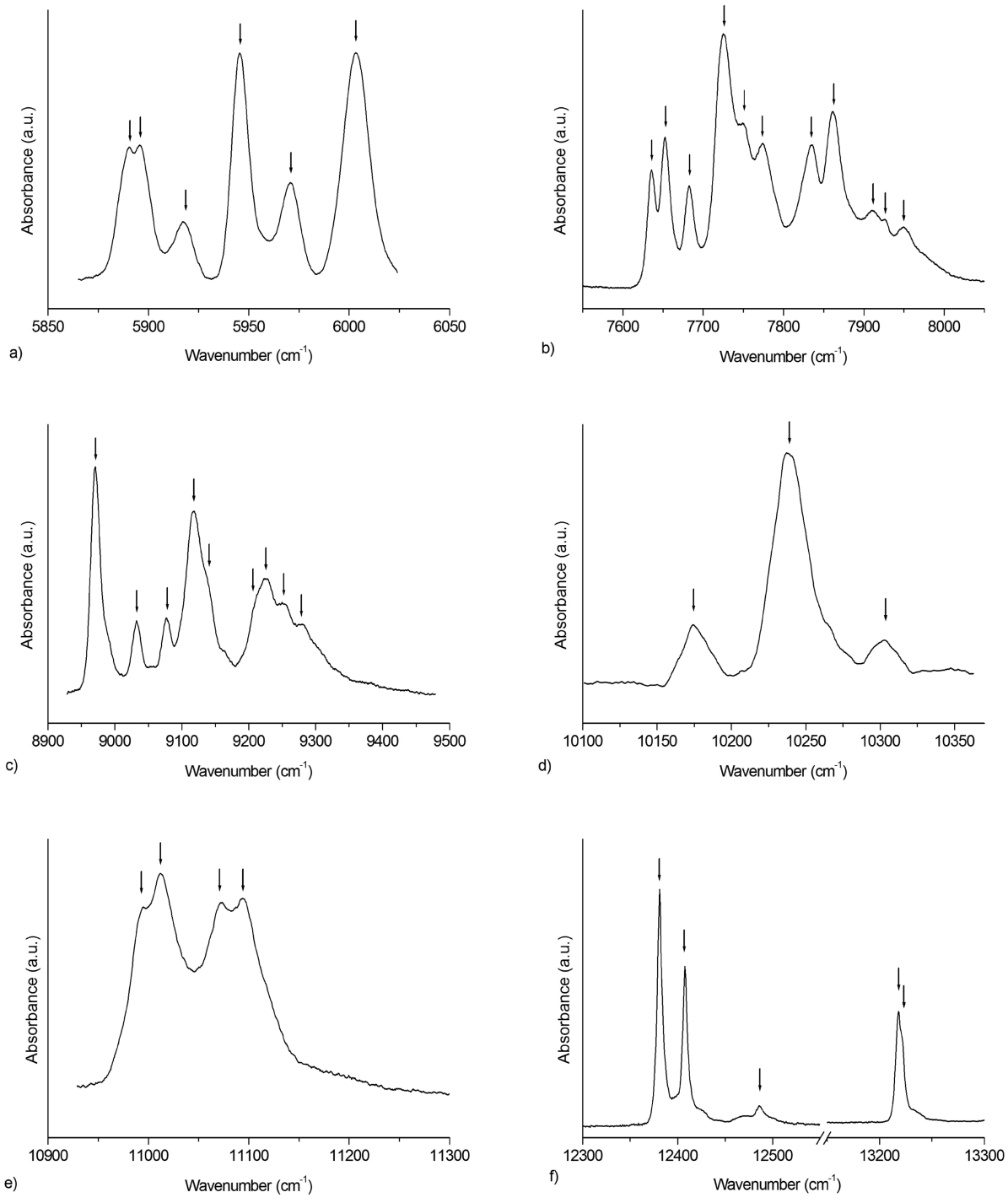

Figure 2. High resolution absorption spectra showing transitions from the ground $^6H_{15/2}$ multiplet to CF components of (a) $^6H_{11/2}$, (b) $^6H_{9/2}$ + $^6F_{11/2}$, (c) $^6H_{7/2}$ + $^6F_{9/2}$, (d) $^6H_{5/2}$, (e) $^6F_{7/2}$, and (f) $^6F_{5/2}$ and $^6F_{3/2}$ excited multiplets of Dy^{3+} in [Dy_2Pd]. Arrows indicate the identified electronic transitions used as the experimental energy levels in CF calculations.

the correspondence between the experimental and the calculated energy levels can be derived from experimental spectra. Therefore, the experimental levels within a given multiplet were ordered according to increasing energy and assigned to the calculated values arranged in an analogous sequence. The number of experimentally identified energy levels was smaller for some multiplets than the number of calculated levels and in such cases the experimental levels were attributed to the calculated ones with the closest energy.

The following fine-tuning procedure has been employed in fittings. For the first fit we used the experimental set of levels preliminarily assigned to the calculated values, based on the levels for which energy could be unambiguously determined from the spectra. In subsequent fits some experimental levels were reassigned and additional energies were included into the procedure. Such optimizing steps were repeated until no further improvement in root-mean-square deviation (*rms*) between the calculated energies and the experimental ones was observed. In the final fit, 38 experimentally determined energy levels were

dx.doi.org/10.1021/ic4021542 | *Inorg. Chem.* 2013, 52, 13199−13206

Table 1. Spherical Polar Coordinates (θ_i, φ_i, R_i) of the Oxygen Ligands (O1−O7) and the Nitrogen Ligand N3 in [Dy_2Pd] Expressed in the Cartesian Axis System (x, y, z) Defined in Figure 3

ligands	θ_i [deg]	φ_i [deg]	R_i [nm]
O1	69.22	123.30	2.276
O2	74.93	−145.40	2.363
O3	77.23	−70.13	2.339
O4	75.81	7.79	2.324
O5	114.08	70.33	2.391
O6	146.69	−26.05	2.353
O7	138.58	173.97	2.337
N3	0.00	0.00	2.584

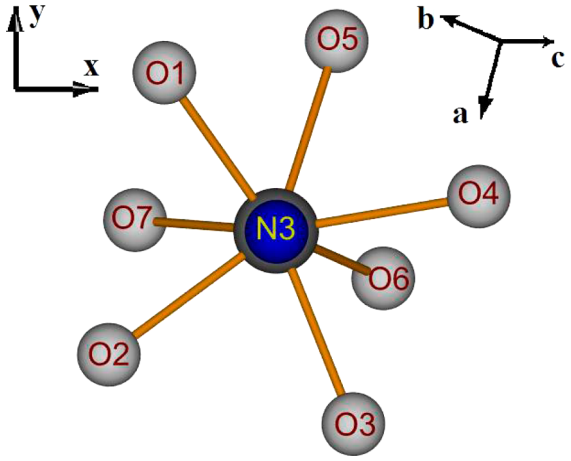

Figure 3. Coordination of Dy^{3+} ions in [Dy_2Pd] represented in the Cartesian axis system (x, y, z) defined in the text; the orientation of the CAS (a, b, c) is also shown.

supplemented with 4 components of the ground $^6H_{15/2}$ multiplet (see text below) and included in the CF analysis.

In the fitting procedure the free ion parameters (FIPs): E_{avg}, F^2, F^4, F^6 and ζ_{4f}, were freely varied, whereas the remaining ones were adopted[17] as for LaF_3:Dy^{3+}. The following CF parameters B_{20}, B_{21}, B_{2-1}, B_{22}, B_{2-2}, B_{40}, and B_{60} were included directly in fittings, whereas the remaining CFPs were expressed via the SPM parameters $B_k(a)$ (for ligand O1), and $B_k(b)$ (for ligands O2−O7), using SPM expression (e.g., eq (8) in ref 14a), R_i distances from Table 1, and the coordination factors $g_{k,q}$ from Supporting Information, Table S3. Thus, the values of B_{20}, B_{21}, B_{2-1}, B_{22}, B_{2-2}, B_{40}, B_{60}, $B_4(a)$, $B_4(b)$, $B_6(a)$, and $B_6(b)$ CF parameters were freely varied in the fitting procedure. The fittings have yielded very satisfactory agreement between the experimental energy levels and the calculated ones (rms = 12.4 cm^{-1}). The values of intrinsic parameters (in cm^{-1}): $B_4(a)$ = 1161, $B_6(a)$ = 124, $B_4(b)$ = 422, and $B_6(b)$ = 290 appear very reasonable. The signs of the CFPs calculated using these fine-tuned values of $B_k(a)$ and $B_k(b)$ and the coordination factors listed in Supporting Information, Table S3 agree well with those predicted by SPM calculations. The fitted FIPs and CFPs are listed in Table 2, column Fit-I. The energy levels and the components of the state vector for the ground multiplet $^6H_{15/2}$ of Dy^{3+} in [Dy_2Pd] obtained using the CFP set Fit-I (see Table 2) are provided in Table 3. A full listing of the corresponding calculated energy levels and the experimental ones for Dy^{3+} ion in [Dy_2Pd] is provided in Supporting Information, Table S4.

Table 2. Fitted Free-Ion and CF Parameters for Dy^{3+} Ions in [Dy_2Pd][a]

	Fit-I[b]	Fit-II[b]		Fit-I[b]	Fit-II[b]
E_{avg}	55618(5)	55808(5)	B_{60}	334(154)	216(142)
F^2	89843(19)	90430(18)	B_{61}	73	41
F^4	65144(32)	64620(31)	B_{6-1}	127	162
F^6	47947(29)	48628(29)	B_{62}	193	165
ζ_{4f}	1905(2)	1904(2)	B_{6-2}	−156	−189
B_{20}	−205(48)	−190(53)	B_{63}	28	−36
B_{21}	−18(19)	−20(17)	B_{6-3}	−46	−55
B_{2-1}	33(24)	−2(25)	B_{64}	63	74
B_{22}	20(23)	5(24)	B_{6-4}	−222	−226
B_{2-2}	43(21)	27(22)	B_{65}	−191	−202
B_{40}	465 (195)	413(205)	B_{6-5}	−26	−110
B_{41}	−164	−180	B_{66}	118	49
B_{4-1}	−42	−16	B_{6-6}	3	−19
B_{42}	294	295	n	42	42
B_{4-2}	−175	−172	rms	12.4	12.0
B_{43}	−820	−852			
B_{4-3}	−206	−212			
B_{44}	−194	−215			
B_{4-4}	575	598			

[a]All values are in cm^{-1}, except for n (dimensionless). Note that B_{20}, B_{21}, B_{2-1}, B_{21}, B_{2-2}, B_{40}, and B_{60} were obtained from direct fittings, whereas the remaining CFPs are calculated using the fine-tuned values of $B_k(a)$ and $B_k(b)$ obtained using the SPM procedure and the coordination factors; for explanations see text. [b]Some of the free-ion parameters were kept at constant values adopted[17] as for LaF_3:Dy^{3+} (in cm^{-1}): α = 18.0, β = −633.0, γ = 1790.0, T^2 = 329.0, T^3 = 36.0, T^4 = 127.0, T^6 = −314.0, T^7 = 404.0, T^8 = 315.0, M^0 = 3.39, M^2 = 1.90, M^4 = 1.29, P^2 = 719.0, P^4 = 539.0, P^6 = 360.0.

Note, that the Dy^{3+} ion site in [Dy_2Pd] has no symmetry elements, thus the formal expansion of the crystal field potential for the f-electron system takes in all 27 parameters B_{kq} (k = 2,4,6; q = −k, ..., k). In general, the number of independent CFPs may be reduced by three by appropriate rotation of coordination system by three Euler angles.[18,19] The method[18] or the 3DD method[20] may be used to eliminate the B_{21}, B_{2-1}, and B_{2-2} parameters. However, to determine the Euler angles required to perform such reduction the reliable values of B_{2q} parameters are necessary, which are not precisely determined before the refining procedure. On the other hand usage of SPM enables to reduce the number of parameters and thus all B_{2q} are included in the fitting procedure employed here.

No splittings of the ground $^6H_{15/2}$ multiplet could be observed in the absorption spectra measured at lower temperatures. Nevertheless, based on hot transitions observed at higher temperatures, the energy of about 40 cm^{-1} may be ascribed to the first split component. On the other hand, the variation of the magnetic susceptibility at lower temperatures depends most strongly on the electronic levels structure lying lowest in energy. Ishikawa et al.[9] have attempted fittings of the three axial CFPs only, that is, neglecting the two tetragonal CFPs, to the experimental magnetic susceptibility $\chi_m T$ curves for [Pc_2Ln]TBA (Ln = Tb, Dy, Ho, Er, Tm, and Yb). However, in the present case of low site symmetry and hence the much greater number of relevant CFPs, this approach is not feasible. Moreover, our experience shows that such fittings usually yield CFP values that reproduce incorrectly the energy levels obtained from the absorption spectra—not only for the excited multiplets but the ground multiplet as well. Hence, we have adopted a more cumbersome but hopefully more reliable

dx.doi.org/10.1021/ic4021542 | Inorg. Chem. 2013, 52, 13199−13206

Table 3. Energy Levels and Components of the State Vector for the Ground Multiplet $^6H_{15/2}$ of Dy^{3+} in $[Dy_2Pd]$ Obtained Using the CFP Set Fit-I/Fit-II

	composition of the wave functions (in %)							
energy levels (cm^{-1})	|±1/2⟩	|±3/2⟩	|±5/2⟩	|±7/2⟩	|±9/2⟩	|±11/2⟩	|±13/2⟩	|±15/2⟩
8/2	**50/41**	21/19	3/6	11/13	9/11	1/3	2/4	2/2
41/32	8/12	22/27	**39/28**	7/8	5/5	14/13	6/6	0/1
130/130	7/11	16/16	11/10	14/12	8/8	5/6	**25/22**	13/14
190/192	10/9	4/4	18/17	11/12	12/12	13/11	12/9	**21/24**
240/244	9/6	12/10	2/1	7/9	4/5	12/14	16/19	**37/34**
293/294	2/1	1/1	13/11	19/15	20/21	**24/22**	13/17	9/12
331/342	9/13	13/14	11/12	13/14	**19/18**	9/8	12/11	13/9
439/426	3/4	6/6	11/12	18/17	**22**/20	21/**22**	14/15	4/4

approach. Several fittings were carried out using several experimental energy level sets consisting of 38 energy levels determined for the excited multiplets from the absorption spectra and several combinations of the four lowest (i.e., in the range of 0−200 cm^{-1}) CF components of the ground multiplet. For each such set the CFPs were fine-tuned using the procedure described above. Then, the wave functions obtained using the final CFP sets were used to calculate the temperature dependence of magnetic susceptibility based on eq 1, and the predicted $\chi_m T$ curves were compared with the experimental ones.

Figure 4 shows the experimental and calculated plots of the molar magnetic susceptibility times temperature (i.e., the

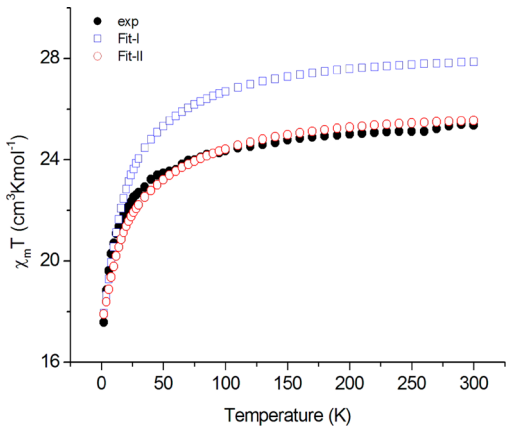

Figure 4. Experimental and calculated temperature dependence of the products $\chi_m T$ for $[Dy_2Pd]$ obtained using the procedure based on eq 2 (Fit-I) or eq 3 (Fit-II).

product $\chi_m T$) versus temperature T for the powder samples of $[Dy_2Pd]$. Analysis of Figure 4 indicates that none of the final CFP sets could satisfactorily describe the experimental $\chi_m T$ curves in the whole temperature range. The CFP set Fit-I in Table 2 yields the best agreement of the theoretical and experimental curves at lower temperatures. This CFP set corresponds to the CF components of the ground multiplet assumed as 0, 35, 150, and 200 cm^{-1}. First we consider the situation when the total molecular magnetic moment may be directly represented as the true sum of the magnetic moments obtained for two independent Dy ions. Then, correspondingly, for the products $\chi_m T$ for $[Dy_2Pd]$ the equation holds

$$\chi_m T(\text{molecule}) = 2 \times \chi_m T(\text{ion}) \quad (2)$$

However, the value of the product $\chi_m T$(total) is 25.4 cm^3 K mol^{-1} at room temperature (300 K), that is, slightly lower than that expected[21] for two isolated Dy(III) ions 28.3 cm^3 K mol^{-1}. Hence, the CF effect and eq 2 cannot account for the observed discrepancy.

Strongly anisotropic Ln compounds often exhibit not fully saturated magnetization and thus susceptibility.[22] This may be partially due to an incomplete field-alignment of the microcrystals. In our case, another reason is also possible, as follows. The molecule has inversion symmetry and accordingly the molecular magnetic moment will be the true sum from each Dy moment since the easy axis is unique in a molecule. One can consider, however, the molecular arrangement in the unit cell with a space group monoclinic $P2_1/n$. The molecules are arranged in a herringbone manner. Hence the bulk data is not a simple sum from the individual molecular values. Strong anisotropy seems to be responsible for SMM properties as well as spin-canted structures.[23] Namely, when an external magnetic field is applied to the easy axis for one molecule, a neighboring molecule feels a transverse field to some extent. Thus a cosine function factor is needed for description of the total molecular magnetic moment. We have assumed that then the total molecular magnetic moment would be the sum of (1) the magnetic moment obtained for one independent Dy ion and (2) this magnetic moment multiplied by the parameter F, which is related to the cosine of the angle between the easy axis for the Dy ions in two nearby molecules in the unit cell. Then, correspondingly, for the products $\chi_m T$ for $[Dy_2Pd]$ the equation, which effectively defines the parameter F, holds:

$$\chi_m T(\text{molecule, avg}) = (\chi_m T(\text{molecule}) + F \times \chi_m T(\text{molecule}))/2 \quad (3)$$

Using the procedure based on eq 3 several fittings were carried out in the same manner as described above for the procedure based on eq 2. The results are presented in Figure 4 (Fit-II).

Analysis of Figure 4 indicates that the best agreement of the theoretical and experimental $\chi_m T$ curves in the whole temperature range is obtained for slightly changed values of the CF components of the ground multiplet: 0, 30, 150, and 200 cm^{-1}, that is, for the CFP set Fit-II in Table 2, while taking the parameter F = 0.835 instead of F = 1. A separate consideration is needed to justify the predicted value of the parameter F in terms of the structural cosine function factor defined above. Note that the CFP sets Fit-I and Fit-II do not differ significantly (see Table 2), whereas the *rms* values are very close in both cases. The energy levels and the components of the state vector for the ground multiplet $^6H_{15/2}$ of Dy^{3+} in $[Dy_2Pd]$ obtained using the CFP set Fit-II (see Table 2) are also provided in Table 3, whereas the full listing of the corresponding calculated energy levels is provided in

dx.doi.org/10.1021/ic4021542 | *Inorg. Chem.* 2013, 52, 13199−13206

Supporting Information, Table S4. Importantly, the calculated energy levels as well as the composition of the wave functions are also very close for both CFP sets: Fit-I and Fit-II (see Supporting Information, Table S4).

DISCUSSION

The recently synthesized complex, [Dy_2Pd], is investigated. This complex, in contrast to many heterometallic 4f-3d compounds with the magnetic 3d ions, for example, [Ln_2Cu] systems, contains instead the diamagnetic Pd ions. Hence, the experimental studies the [Dy_2Pd] complex, which is isostructural with [Dy_2Cu], may shed light on the peculiarities of the observed behavior of the related isostructural [Ln_2Cu] systems. In this study the [Dy_2Pd] complex, which exhibits low site symmetry around Dy^{3+} ions, has been investigated by the optical absorption spectroscopy at 4.2 K and temperature dependence of magnetic susceptibility in the range 1.8−300 K. The motivation for this study is to provide grounds for explanation of the antiferro- and ferro-magnetic couplings between the 4f and 3d(4d) ions in this class of systems, which have been intensively studied for development of novel single-molecular magnets (SMMs). For this purpose we have determined the experimental energy levels of Dy^{3+} ions in the powder [Dy_2Pd] sample from the absorption spectra and rationalized them by the CF analysis in a manner consistent with results for other such complexes. In view of the low site symmetry, the large number of freely varied parameters exists and hence in the fitting procedure some of the FIPs have been restricted to literature values, whereas the CF parameters have been restricted using the superposition model. The fittings yielded very satisfactory agreement between the experimental and the calculated energy levels with the *rms* of about 12 cm^{-1}. The energies and exact composition of the state vector for the ground multiplet $^6H_{15/2}$ of Dy^{3+} have also been determined.

The results of the CF analysis serve as an input for the simulation of the temperature dependence of the magnetic susceptibility and thus enable the theoretical interpretation of the experimentally measured magnetic susceptibility for the [Dy_2Pd] complex. In the low-temperature region the variation of the product $\chi_m T$ depends on the depopulation of Stark sublevels of the ground $^6H_{15/2}$ of Dy^{3+} multiplet and can be accurately modeled by the CF effect. To obtain the acceptable agreement in the whole temperature range, the parameter F, which is related to the cosine of the angle between the easy axis for the Dy^{3+} ions in two nearby molecules in the unit cell, has been employed. The best agreement of the theoretical and experimental $\chi_m T$ curves in the whole temperature range is obtained for the CF components of the ground $^6H_{15/2}$ multiplet fitted as 0, 30, 150, and 200 cm^{-1}, while taking the parameter $F = 0.835$ instead of $F = 1$. The CF parameter sets obtained using two approaches, that is, $F = 1$ and $F < 1$, do not differ significantly, whereas the *rms* values are very close in both cases. The energy levels and the components of the state vector for the ground multiplet $^6H_{15/2}$ of Dy^{3+} in [Dy_2Pd] obtained in both approaches are also very close. Although the temperature dependence of magnetic susceptibility is not ideally described, the achieved agreement is fully satisfactory since the final fitted CF parameters and the corresponding wave functions enable reasonable simulation simultaneously of the energy levels of the ground and excited multiplets as well as the temperature dependence of the magnetic susceptibility.

The aspect which requires further studies concerns the possible justification of the predicted value of the parameter F in terms of the structural cosine function factor. The question about the difference between the room temperature value of the product $\chi_m T$ 25.4 cm^3 K mol^{-1} at 300 K, slightly lower than the expected 28.3 cm^3 K mol^{-1} for two isolated Dy(III) ions, remains still open. The tentative explanations based on the assumption that the total magnetic moment depends on the relative orientation of the two [Dy_2Pd] molecules in the elementary cell needs to be independently corroborated or alternative explanations based on other effects must be sought. Note that a similar behavior of the product $\chi_m T$ as for [Dy_2Pd] is also observed in [Dy_2Cu], where the measurements were carried out at present only up to 100 K, whereas in the case of [Dy_2Ni] the value close to the expected one (∼28 cm^3 K mol^{-1}) is obtained. Adding the nickel(II) contribution (ca. 1 cm^3 K mol^{-1}) to the total magnetic moment, a slight discrepancy may be found. It is expected that the polycrystalline (or powder) data often exhibit such discrepancy[22], whereas the incomplete field-alignment seems to become a non-negligible reason and thus application of the parameter F defined in eq 3 appears inevitable in such cases.

In short, this study provides grounds for subsequent investigation of the magnetic exchange interactions in the pertinent heterometallic complexes. The CF parameters obtained here appear very reliable, since they reproduce the experimental spectroscopic data very well. An important and difficult question now is to meaningfully utilize the present results for interpretation of the magnetic properties of the [Dy_2Pd] and related samples. Further work in this direction is now in progress

ASSOCIATED CONTENT

Supporting Information

Tables containing the crystallographic coordinates of atoms, the coordination factors, and the experimental and calculated energy levels for Dy^{3+} ion in [Dy_2Pd]. This material is available free of charge via the Internet at http://pubs.acs.org.

AUTHOR INFORMATION

Corresponding Author

*E-mail: miroslaw.karbowiak@chem.uni.wroc.pl.

Notes

The authors declare no competing financial interest.

ACKNOWLEDGMENTS

This work was partly supported by KAKENHI (Grant Numbers JSPS/22350059 and 23750056 and MEXT/23110711). One of us (C.Z.R.) would like to thank Prof. Hiroyuki Nojiri, Institute for Materials Research, Tohoku University, Sendai, Japan, for the Visiting Professorship in his group in the period Oct 1−Nov 31, 2011, which provided an opportunity to start this research project, as well as for superb hospitality.

REFERENCES

(1) (a) Christou, G.; Gatteschi, D.; Hendrickson, D. N.; Sessoli, R. *MRS Bull.* **2000**, *25*, 66−71. (b) Aromi, G.; Brechin, E. K. *Struct. Bonding (Berlin)* **2006**, *122*, 1−67. (c) Christou, G. *Polyhedron* **2005**, *24*, 2065−2075.

(2) (a) Sessoli, R.; Tsai, H. L.; Schake, A. R.; Wang, S.; Vincent, J. B.; Folting, K.; Gatteschi, D.; Christou, G.; Hendrickson, D. N. *J. Am. Chem. Soc.* **1993**, *115*, 1804−1816. (b) Sessoli, R.; Gatteschi, D.; Caneschi, A.; Novak, M. A. *Nature* **1993**, *365*, 141−143.

(3) Christou, G. *Polyhedron* **2005**, *24*, 2065−2075.

(4) Sorace, L.; Benelli, C.; Gatteschi, D. *Chem. Soc. Rev.* **2011**, *40*, 3092−3104.
(5) Andruh, M.; Ramade, I.; Codjovi, E.; Guillou, O.; Kahn, O.; Trombeet, J. C. *J. Am. Chem. Soc.* **1993**, *115*, 1822−1829.
(6) Ishikawa, N.; Iino, T.; Kaizu, Y. *J. Phys. Chem. A* **2002**, *106*, 9543−9550.
(7) (a) Baldovi, J. J.; Cardona-Serra, S.; Clemente-Juan, J. M.; Coronado, E.; Gaita-Ariño, A. *Chem. Sci.* **2013**, *4*, 938−946. (b) Baldoví, J. J.; Cardona-Serra, S.; Clemente-Juan, J. M.; Coronado, E.; Gaita-Ariño, A. *Inorg. Chem.* **2012**, *51*, 12565−12574. (c) Baldovi, J. J.; Borrás-Almenar, J. J.; Clemente-Juan, J. M.; Coronado, E.; Gaita-Ariño, A. *Dalton Trans.* **2012**, *41*, 13705−13710. (d) Cardona-Serra, S.; Clemente-Juan, J. M.; Coronado, E.; Gaita-Ariño, A.; Camón, A.; Evangelisti, M.; Luis, F.; Martínez-Pérez, M. J.; Sese, J. *J. Am. Chem. Soc.* **2012**, *134*, 14982−14990.
(8) Andruh, M.; Costes, J. P.; Diaz, C.; Gao, S. *Inorg. Chem.* **2009**, *48*, 3342−3359.
(9) Ishikawa, N.; Sugita, M.; Okubo, T.; Takana, N.; Iino, T.; Kaizu, Y. *Inorg. Chem.* **2003**, *42*, 2440−2446.
(10) (a) Okazawa, A.; Watanabe, R.; Nezu, M.; Shimada, T.; Yoshii, S.; Nojiri, H.; Ishida, T. *Chem. Lett.* **2010**, *39*, 1331−1332. (b) Okazawa, A.; Nogami, T.; Nojiri, H.; Ishida, T. *Inorg. Chem.* **2008**, *47*, 9763−9765. (c) Okazawa, A.; Nogami, T.; Nojiri, H.; Ishida, T. *Inorg. Chem.* **2009**, *48*, 3292. For the nickel(II) analogues, see also: (d) Okazawa, A.; Shimada, T.; Kojima, T.; Yoshii, S.; Nojiri, H.; Ishida, T. *Inorg. Chem.* **2013**, DOI: 10.1021/ic402417h.
(11) (a) Ishida, T.; Watanabe, R.; Fujiwara, K.; Okazawa, A.; Kojima, N.; Tanaka, G.; Yoshii, S.; Nojiri, H. *Dalton Trans.* **2012**, *41*, 13609−13619. (b) for the 2p-4f systems, see: Ishida, T.; Murakami, R.; Kanetomo, T.; Nojiri, H. *Polyhedron* **2013** in press; DOI: 10.1016/j.poly.2013.04.004.
(12) (a) Mori, F.; Nyui, T.; Ishida, T.; Nogami, T.; Choi, K.-Y.; Nojiri, H. *J. Am. Chem. Soc.* **2006**, *128*, 1440−1441. (b) Ueki, S.; Ishida, T.; Nogami, T.; Choi, K.-Y.; Nojiri, H. *Chem. Phys. Lett.* **2007**, *440*, 263−267.
(13) (a) Rinehart, J. D.; Long, J. R. *Chem. Sci.* **2011**, *2*, 2078−2085. (b) Murakami, R.; Ishida, T.; Yoshii, S.; Nojiri, H. *Dalton Trans.* **2013**, *42*, 13968−13973.
(14) (a) Karbowiak, M.; Gnutek, P.; Rudowicz, C. *Phys. B* **2010**, *405*, 1927−1940. (b) Karbowiak, M.; Rudowicz, C.; Gnutek, P. *Opt. Mater.* **2011**, *33*, 1147−1161. (c) Karbowiak, M.; Rudowicz, C. *Chem. Phys.* **2011**, *383*, 68−82. (d) Karbowiak, M.; Gnutek, P.; Rudowicz, C.; Ryba-Romanowski, W. *Chem. Phys.* **2011**, *387*, 69−78. (e) Karbowiak, M.; Gnutek, P.; Rudowicz, C. *Spectrochim. Acta A* **2012**, *87*, 46−60. (f) Karbowiak, M.; Gnutek, P.; Rudowicz, C. *Chem. Phys.* **2012**, *400*, 29−38. (g) Karbowiak, M.; Cichos, J.; Rudowicz, C. *J. Phys. Chem. A* **2012**, *116*, 10574−10588.
(15) Okazawa, A.; Nojiri, H.; Ishida, T.; Kojima, N. *Polyhedron* **2011**, *30*, 3140−3144.
(16) Van Vleck, J. V. *J. Appl. Phys.* **1968**, *39*, 365−372.
(17) Carnall, W. T.; Goodman, G. L.; Rajnak, K.; Rana, R. S. *J. Chem. Phys.* **1989**, *90*, 3443−3457.
(18) Burdick, G. W.; Reid, M. F. *Mol. Phys.* **2004**, *102*, 1141−1147.
(19) Mech, A.; Gajek, Z.; Karbowiak, M.; Rudowicz, C. *J. Phys.: Condens. Matter* **2008**, *20* (385205), 1−13.
(20) Gnutek, P.; Rudowicz, C. *Opt. Mater.* **2008**, *31*, 391−400.
(21) Suzuki, K.; Sato, R.; Mizuno, N. *Chem. Sci.* **2013**, *4*, 596−600.
(22) (a) Costes, J.-P.; Auchel, M.; Dahan, F.; Peyrou, V.; Shova, S.; Wernsdorfer, W. *Inorg. Chem.* **2006**, *45*, 1924−1934. (b) Lin, P.-H.; Burchell, T. J.; Clerac, R.; Murugesu, M. *Angew. Chem., Int. Ed.* **2008**, *47*, 8848−8851.
(23) Miyasaka, H.; Nakata, K.; Lecren, L.; Coulon, C.; Nakazawa, Y.; Fujisaki, T.; Sugiura, K.-i.; Yamashita, M.; Clerac, R. *J. Am. Chem. Soc.* **2006**, *128*, 3770−3783.